

Magnetization nutation induced by surface effects in nanomagnets

R. Bastardis,^{*} F. Vernay,[†] and H. Kachkachi[‡]

*Laboratoire PROMES CNRS (UPR-8521) & Université de Perpignan Via Domitia,
Rambla de la thermodynamique, Tecnosud, 66100 Perpignan, France*

(Dated: March 4, 2022)

We investigate the magnetization dynamics of ferromagnetic nanoparticles in the atomistic approach taking account of surface anisotropy and the spin misalignment it causes. We demonstrate that such inhomogeneous spin configurations induce nutation in the dynamics of the particle's magnetization. More precisely, in addition to the ordinary precessional motion with frequency $f_p \sim 10$ GHz, we find that the dynamics of the net magnetic moment exhibits two more resonance peaks with frequencies f_c and f_n which are higher than the frequency f_p : $f_c = 4 \times f_p \sim 40$ GHz is related with the oscillations of the particle's magnetic moment between the minima of the effective potential induced by weak surface anisotropy. On the other hand, the much higher frequency $f_n \sim 1$ THz is attributed to the magnetization fluctuations at the atomic level driven by exchange interaction. We have compared our results on nutation induced by surface effects with those rendered by the macroscopic approach based on the Landau-Lifshitz-Gilbert equation augmented by an inertial term (proportional to the second-order time derivative of the macroscopic moment) with a phenomenological coefficient. The good agreement between the two models have allowed us to estimate the latter coefficient in terms of the atomistic parameters such as the surface anisotropy constant. We have thus proposed a new origin for the magnetization nutations as being induced by surface effects and have interpreted the corresponding resonance peaks and their frequencies.

I. INTRODUCTION

Research on nanoscale magnetic materials benefits from a continuing impetus owing to an increasing demand of our modern societies for ever smaller devices with ever higher storage densities and faster access times. These devices are the upshot of spintronics or magnonic applications with materials exhibiting thermally stable magnetic properties, energy efficient magnetization dynamics, and controlled fast magnetization switching. In the macroscopic approach, the magnetization dynamics on time scales ranging from microseconds to femtoseconds can be described by the Landau-Lifshitz-Gilbert (LLG) equation [1–3]

$$\frac{d\mathbf{m}}{dt} = \mathbf{m} \times \left(\gamma \mathbf{H}_{\text{eff}} - \frac{\alpha}{m} \frac{d\mathbf{m}}{dt} \right) \quad (1)$$

where \mathbf{H}_{eff} is the effective field acting on the macroscopic magnetic moment \mathbf{m} carried by the nanomagnet, γ the gyromagnetic factor and α the phenomenological damping parameter. Equation (1) describes the relaxation of \mathbf{m} towards \mathbf{H}_{eff} while maintaining a constant magnitude, *i.e.* $\|\mathbf{m}\| = m$, assuming that the nanomagnet is not coupled to any heat bath or other time-dependent external perturbation. The first term on the right hand of Eq. (1) describes the precessional motion of the magnetic moment \mathbf{m} around the effective field \mathbf{H}_{eff} . This is well known from the classical mechanics of a gyroscope. Indeed, if an external force tilts the rotation axis of the gyroscope away from the direction of the gravity field, the rotation axis no longer coincides with the angular-momentum direction. The consequence is an additional movement of the gyroscope around the axis of the angular

momentum. This motion is called *nutation*. In the case of the magnetic moment \mathbf{m} , this additional motion (nutation) can occur if the effective field \mathbf{H}_{eff} becomes time-dependent. Indeed, in the presence of a time-dependent magnetic field (rf or microwave field), there appears the fundamental effect of transient nutations which has been widely investigated in NMR [4], EPR [5, 6], and optical resonance [7], see also the review by Fedoruk [8]. Magnetic or spin nutation was first predicted in Josephson junctions [9–13] and was later developed using various approaches based on first principles [14], electronic structure theory [15–19], or in a macrospin approach where the LLG equation (1) is extended by a second-order time derivative [20–23].

Magnetic nutation may also occur at the level of atomic magnetic moments on ultra-short time scales. For instance, in Ref. 24 it is argued that nutation is enhanced for atomic spins with low coordination numbers and that it occurs on a time scale of the magnetic exchange energy, *i.e.* a few tens of femtoseconds. More generally this spin nutation is caused by a nonuniform spin configuration which leads to an inhomogeneous effective field \mathbf{H}_{eff} whose magnitude and orientation are different for different lattice sites. These spatial inhomogeneities are a typical result of surface effects that become very acute in nanoscale magnetic systems such as magnetic nanoparticles. In this work we adopt this atomistic approach and show that for a magnetic nanoparticle regarded as a many-spin system, a model henceforth referred to as the *many-spin problem* (MSP), surface effects do induce nutations of the net magnetic moment of the nanoparticle. More precisely, this approach involves at least three energy scales, namely the core (magneto-crystalline) anisotropy, the surface anisotropy

and exchange coupling. Consequently, there appear at least three different frequencies: the lowest corresponds to the ordinary precession around a fixed axis with a constant projection of the net magnetic moment on the latter and the other two frequencies correspond to nutations with a time-dependent projection of \mathbf{m} . In the limiting case of weak surface effects, inasmuch as the spin configuration inside of the nanomagnet can be regarded as quasi-collinear, the dynamics of the nanomagnet can be described with the help of an effective macroscopic model for the net magnetic moment of the nanomagnet. This model will be referred to in the sequel as the *effective one-spin problem* (EOSP). More precisely, it has been shown that a many-spin nanomagnet of a given lattice structure and energy parameters (on-site core and surface anisotropy, local exchange interactions) can approximately be modeled by a macroscopic magnetic moment \mathbf{m} evolving in an effective potential [25] that comprises second and fourth powers of the components $m_\alpha, \alpha = x, y, z$. Within this approach we find two precession frequencies f_p and f_c : f_p corresponds to the precession of \mathbf{m} around the reference z axis with constant m_z and f_c to the frequency of oscillations of \mathbf{m} between the 4 minima of the effective potential produced by its quartic term. When surface or boundary effects are too strong, the spin configuration can no longer be considered as quasi-collinear and thereby the effective model is no longer a good approximation, one has to take account of higher-order fluctuations of the atomic spins. Doing so numerically, we find an additional nutation frequency f_n which is much higher than f_p and f_c as it corresponds to a movement of the atomic spins that occurs at the time scale of the magnetic exchange interaction.

Observation of nutation in magnetization dynamics is difficult because the effect is rather small and the corresponding frequency is beyond the detection capabilities of standard techniques using the magnetization resonance such as the standard FMR or a network analyzer with varying frequency. Nevertheless, from the high-frequency FMR (115 – 345 GHz) spectra obtained for ultra-fine cobalt particles, the authors of Ref. 26 inferred low values for the transverse relaxation time τ_\perp (two orders of magnitude smaller than the bulk value) and suggested that this should be due to inhomogeneous precession which possibly originates from surface spin disorder. Likewise, in Ref. 24 it was shown that nutation in magnetization dynamics of nanostructures occurs at edges and corners, with a much smaller amplitude than the usual precession. More recently, Li *et al.* [27] performed HF-FMR measurements of the effective magnetic field and showed that there was an additional contribution which is quadratic in frequency as obtained from the additional term $d^2\mathbf{m}/dt^2$ in the LLG equation [28, 29].

To sum up, in this work we first demonstrate that surface effects or, more generally, non-collinear atomic spin ordering induce nutation in the magnetization dynamics

of a nanomagnet. Second, it establishes a clear connection between nutation within our atomistic approach and that described by the quadratic frequency dependence of the effective field as described within the macroscopic approach including magnetization inertia. If we cannot provide an analytical connection between the corresponding parameters, we do provide a numerical correspondence between the phenomenological parameter of the macroscopic approach and our atomistic parameters such as the surface anisotropy constant. We also propose an intermediate macroscopic model which accounts for all three resonance frequencies. Finally, we speculate that the resonance peak at f_c , induced by surface effects, provides a route for observing nutation in well prepared assemblies of nanomagnets.

The paper is organized as follows: in Section II we present our model of many-spin nanomagnets, discuss the effects of surface anisotropy on the magnetization dynamics, and present our main results showing two new resonance peaks which we attribute to two kinds of magnetization nutation. In Subsection II A we also discuss a particular situation where it is possible to analytically derive the equation of motion of the net magnetic moment of the (many-spin) nanomagnet which makes it clear that nutation is related with the spin fluctuations at the atomic level. In Subsection II B we compare our results with other works in the literature mostly based on the macroscopic approach using the Landau-Lifshitz-Gilbert equation augmented by an inertial term, and establish a quantitative relationship between the corresponding sets of parameters. Finally, in Section III we summarize the main results of this work and then discuss the possibility to observe the magnetization nutations in resonance experiments.

II. MODEL AND HYPOTHESIS

We consider a nanomagnet with \mathcal{N} atomic spins \mathbf{s}_i on a simple cubic lattice described by the (classical) Hamiltonian ($\|\mathbf{s}_i\| = 1$)

$$\mathcal{H} = -\frac{1}{2} \sum_{i,j} J_{ij} \mathbf{s}_i \cdot \mathbf{s}_j - \mathbf{h} \cdot \sum_{i=1}^{\mathcal{N}} \mathbf{s}_i - \sum_{i=1}^{\mathcal{N}} \mathcal{H}_{\text{an},i} \quad (2)$$

where $\mathbf{h} = \mu_a \mathbf{H}$, μ_a is the magnetic moment associated with the atomic spin, \mathbf{H} is the magnetic field, J_{ij} is the exchange interaction (that may be different for core-surface, surface-surface and core-core links), and $\mathcal{H}_{\text{an},i}$ is the anisotropy energy at site i , a function of \mathbf{s}_i satisfying the symmetry of the problem. More precisely, $\mathcal{H}_{\text{an},i}$ is the energy of on-site anisotropy which is here taken as uniaxial for core spins and of Néel's type for surface spins [30], *i.e.*

$$\mathcal{H}_{\text{an},i} = \begin{cases} -K_c (\mathbf{s}_i \cdot \mathbf{e}_z)^2, & i \in \text{core} \\ +\frac{1}{2}K_s \sum_{j \in \text{n.n.}} (\mathbf{s}_i \cdot \mathbf{e}_{ij})^2, & i \in \text{surface}, \end{cases} \quad (3)$$

where \mathbf{e}_{ij} is the unit vector connecting the nearest neighbors at sites i and j and $K_c > 0$ and $K_s > 0$ are respectively the core and surface anisotropy constants.

The spin dynamics is described by the Landau-Lifshitz equation (LLE) for the atomic spin \mathbf{s}_i

$$\frac{d\mathbf{s}_i}{d\tau} = \mathbf{s}_i \times \mathbf{h}_{\text{eff},i} - \alpha \mathbf{s}_i \times (\mathbf{s}_i \times \mathbf{h}_{\text{eff},i}), \quad (4)$$

with the (normalized) local effective field $\mathbf{h}_{\text{eff},i}$ acting on \mathbf{s}_i being defined by $\mathbf{h}_{\text{eff},i} = -\delta\mathcal{H}/\delta\mathbf{s}_i$; τ is the reduced time defined by

$$\tau \equiv \frac{t}{\tau_s}, \quad (5)$$

where $\tau_s = \mu_a/(\gamma J)$ is a characteristic time of the system's dynamics. By way of example, for cobalt $J = 8$ meV leading to $\tau_s = 70$ fs. Henceforth, we will only use the dimensionless time τ . In these units, $\mathbf{h}_{\text{eff},i} = \mu_a \mathbf{H}_{\text{eff},i}/J$.

Equation (4) is a system of $2\mathcal{N}$ coupled equations for the spins \mathbf{s}_i , $i = \{1, \dots, \mathcal{N}\}$. In this work, it is solved using iterative optimized second-order methods using Heun's algorithm.

The particle's net magnetic moment is defined as

$$\mathbf{s}_0 = \frac{1}{\mathcal{N}} \sum_{i=1}^{\mathcal{N}} \mathbf{s}_i. \quad (6)$$

Next, we introduce the verse of \mathbf{s}_0

$$\mathbf{m} \equiv \frac{1}{s_0} \mathbf{s}_0, \quad s_0 = \left\| \frac{1}{\mathcal{N}} \sum_i \mathbf{s}_i \right\|. \quad (7)$$

As discussed in the introduction, because of surface effects or spatial inhomogeneities of the effective field (mainly due to the fact that the anisotropy constant and the easy axis depend on the lattice site), the spin configuration is not uniform, for an arbitrary set of energy parameters. As a consequence, the vectors \mathbf{s}_i are not all parallel to each other and as such we may define their deviation from the direction \mathbf{m} as [31]

$$\mathbf{s}_i = (\mathbf{m} \cdot \mathbf{s}_i) \mathbf{m} + \boldsymbol{\psi}_i$$

where we have introduced the vector

$$\boldsymbol{\psi}_i \equiv \mathbf{s}_i - (\mathbf{m} \cdot \mathbf{s}_i) \mathbf{m}.$$

It can be easily checked that $\boldsymbol{\psi}_i$ is perpendicular to \mathbf{s}_i , *i.e.* $\boldsymbol{\psi}_i \cdot \mathbf{s}_i = 0 = \boldsymbol{\psi}_i \cdot \mathbf{m}$ and satisfies $\sum_{i=1}^{\mathcal{N}} \boldsymbol{\psi}_i =$

0. This means that the transverse vector $\boldsymbol{\psi}_i$ contains the Fourier components with $\mathbf{k} \neq \mathbf{0}$ and describes spin waves in the nanomagnet. Whereas in the standard spin wave theory \mathbf{s}_0 is a constant corresponding to the ground-state orientation, here it is treated as a time-dependent variable.

Note that using the condition $\|\mathbf{s}_i\| = 1$, we may write $\mathbf{s}_i = \mathbf{m} \sqrt{1 - \boldsymbol{\psi}_i^2} + \boldsymbol{\psi}_i$. Now, in the realistic case, $K_s \ll J$, the deviations of \mathbf{s}_i from the homogeneous state \mathbf{m} are small and one can adopt the following approximation

$$\mathbf{s}_i \simeq \mathbf{m} \left(1 - \frac{1}{2} \boldsymbol{\psi}_i^2 \right) + \boldsymbol{\psi}_i \equiv \mathbf{m} + \delta \mathbf{s}_i$$

where

$$\delta \mathbf{s}_i \equiv -\frac{1}{2} \boldsymbol{\psi}_i^2 \mathbf{m} + \boldsymbol{\psi}_i. \quad (8)$$

Then, we define the magnetization deficit due to surface anisotropy as follows

$$\Delta m \equiv -\frac{1}{\mathcal{N}} \sum_i \mathbf{m} \cdot \delta \mathbf{s}_i. \quad (9)$$

Using Eq. (8) and $\sum_{i=1}^{\mathcal{N}} \boldsymbol{\psi}_i = \mathbf{0}$ we obtain

$$\Delta m = \frac{1}{2\mathcal{N}} \sum_i \boldsymbol{\psi}_i^2 = 1 - \frac{1}{\mathcal{N}} \sum_i (\mathbf{m} \cdot \mathbf{s}_i) = 1 - s_0. \quad (10)$$

In what follows, we will show that the magnetization nutations are a consequence of the magnetization deficit Δm (which is due to the transverse spin fluctuations $\boldsymbol{\psi}_i$) with respect to \mathbf{s}_0 . In order to study nutation, we compute $\Delta m(\tau)$ or the components $m_\alpha(\tau)$, with $\alpha = x, y, z$. In the sequel, we will mainly study the latter as their behavior clearly illustrates the precession and nutation phenomena. In the next section we present a sample of our results obtained for a cube-shaped nanomagnet described by the Hamiltonian (2) together with the anisotropy model in Eq. (3).

A. Magnetization nutation induced by surface anisotropy

In order to clearly illustrate the central result of this work, namely that spin noncollinearities, induced by surface anisotropy, lead to nutation in the magnetization dynamics of a nanomagnet, we consider a simple shape, *e.g.* a cube. Today, nanocubes (of iron or cobalt) are routinely investigated in experiments since their synthesis has become fairly well controlled [32–37]. Here we consider a nanocube of $\mathcal{N} = 729$ spins located on the vertices of a simple cubic lattice (*i.e.* $N_x = N_y = N_z = 9$). This choice has the main advantage that the number of core spins ($\mathcal{N}_c = 343$) is comparable to that of surface

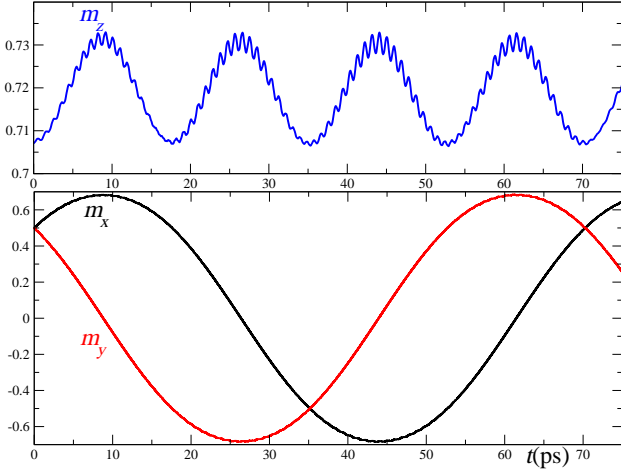


Figure 1: Time evolution of the average magnetization components (m_x , m_y , m_z) for a nanomagnet of $\mathcal{N} = 9 \times 9 \times 9 = 729$ spins with uniaxial anisotropy in the core and Néel surface anisotropy on the surface.

spins ($\mathcal{N}_s = 386$), a configuration suitable for studying the role of surface effects versus core properties. Then, we compute the time evolution of the net magnetic moment \mathbf{m} by solving the system of equations (4), using Eqs. (6) and (7). We start from the initial state $\mathbf{s}_i(t=0) = (1/2, 1/2, 1/\sqrt{2})$ which corresponds to all spins tilted to the same angle with respect to the z axis of the laboratory frame.

Let us first consider the case of a nanocube with anisotropy energy defined in Eq. (3), *i.e.* uniaxial for core spins and of Néel's type for surface ones. A surface spin is defined as the spin whose coordination number is smaller than in the core (here 6 on a simple cubic lattice). For simplicity, we set all exchange couplings equal to a reference value J everywhere in the core, on the surface and at the interface between them, *i.e.* $J_{cc} = J_{cs} = J_{ss} = J$. All energy constants are then measured in units of J , so that $J = 1$ and $k_c \equiv K_c/J = 0.001$, $k_s \equiv K_s/J = 0.01$. These are typical values extracted from experiments on cobalt and iron nanoparticles [38–40]. In this calculation, the external magnetic field and damping are both set to zero.

Solving the LLE (4) renders the components of $\mathbf{m}(\tau)$ defined in Eq. (7). These are shown in Fig. 1. In the lower panel, $m_x(\tau)$ and $m_y(\tau)$ show the usual precessional movement of $\mathbf{m}(\tau)$ around the z axis. The corresponding frequency for the parameters given above is $f_p = 14$ GHz. If $\mathbf{m}(\tau)$ were to exhibit only this precession, its component $m_z(\tau)$ would be a constant with a constant tilt angle between $\mathbf{m}(\tau)$ and the z axis. However, as can be seen in the upper panel, it is clearly not the case. Indeed, we see a double modulation of $m_z(\tau)$ in time; there are two oscillations: i) one with frequency $f_c = 4 \times f_p = 56$ GHz and an amplitude that is an order of magnitude smaller than precession, and ii) another os-

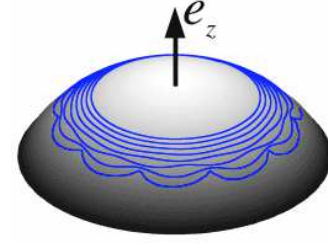


Figure 2: Illustration of the nutation of the macrospin \mathbf{s}_0 in the presence of damping ($\alpha \neq 0$). We have used nonzero damping for later reference.

cillation with the much higher frequency $f_n = 1.1$ THz and an amplitude two orders of magnitude smaller than precession. These oscillations are further illustrated in Fig. 2.

Let us now discuss the origin of these oscillations. As discussed in the introduction, in the case of not-too-strong surface effects, the MSP may be mapped onto an EOSP [25, 41–43] for the net magnetic moment \mathbf{m} of the particle evolving in an effective potential containing a quadratic and a quartic term in the components of \mathbf{m} . This work has recently been extended to cube-shaped magnets [44]. So for a nanomagnet within the EOSP approach the equation of motion reads

$$\frac{d\mathbf{m}}{d\tau} = \mathbf{m} \times [2k_2 m_z \mathbf{e}_z - 4k_4 (m_z^3 \mathbf{e}_z + m_y^3 \mathbf{e}_y + m_x^3 \mathbf{e}_x)]. \quad (11)$$

Here $z = 6$ is the coordination number and $k_2 = k_c \mathcal{N}_c / \mathcal{N}$. For a sphere $k_4 = \kappa k_s^2 / zJ$ where κ is a surface integral [25], and for a cube we have $k_4 = (1 - 0.7/\mathcal{N}^{1/3})^4 k_s^2 / zJ$ [44].

The components $m_\alpha(\tau)$ rendered by Eq. (11) exhibit two resonance peaks corresponding to: i) the ordinary precession with frequency f_p and ii) the oscillation with frequency f_c between the minima of the effective potential induced by the term in k_4 . The latter is due to the fact that the effective magnetic moment has now to explore a potential-energy surface that comprises four saddle points because of the cubic anisotropy (with constant k_4). Therefore, m_z visits a minimum each time \mathbf{m} passes over one of these saddle points, and this occurs with the frequency $f_c = 4 \times f_p = 56$ GHz. Thus, f_c is a consequence of the first correction stemming from (relatively weak) surface effects.

In the case of larger values of k_s and thereby stronger spin noncollinearities, it is no longer possible to map the many-spin particle onto an effective particle. One then has to fully deal with the spin fluctuations. As a consequence it is no longer an easy matter to derive an equation of motion similar to Eq. (11) in the general case. Nevertheless, in Ref. 31 two relatively simpler configurations of anisotropy were studied, namely a uniform

uniaxial anisotropy (with the same constant and orientation) or a random anisotropy (with the same constant and random orientation). It was then possible to derive a system of (coupled) equations for $\mathbf{m}(t)$ and $\boldsymbol{\psi}_i(t)$ containing higher-order terms in $\boldsymbol{\psi}_i(t)$, see Eqs. (21) and (26) in Ref. 31. In the present situation with a nonuniform anisotropy configuration, these higher-order contributions are responsible for the nutation movement with frequency f_n , as they lead to a net magnetization deficit, see Eq. (10) and Fig. 3 where the plot of Δm shows such a movement. More precisely, these fluctuations of the atomic spins lead to a precession of the latter around their local effective field $\mathbf{h}_{\text{eff},i}$ that evolves in time due to exchange interaction. Unfortunately, in this complex situation it is a rather difficult task to derive an explicit expression for $\mathbf{h}_{\text{eff},i}$ and thereby an analog of Eq. (11). However, we may consider a simpler model of a nanomagnet with a uniaxial anisotropy having the easy axis along \mathbf{e}_z for all sites, but with a constant that is different in the core from that on the surface, *i.e.* $\mathbf{e}_i \parallel \mathbf{e}_z$, $k_c \neq k_s$. Therefore, instead of the model in Eq. (3) we consider the following one

$$\mathcal{H}_{\text{an},i} = \begin{cases} -k_c (\mathbf{s}_i \cdot \mathbf{e}_z)^2, & i \in \text{core}, \\ -k_s (\mathbf{s}_i \cdot \mathbf{e}_z)^2, & i \in \text{surface}. \end{cases} \quad (12)$$

This configuration is quite plausible especially in elongated nanomagnets such as nanorods [45] and nanowires [46] where the magnetostatic energy is strong enough to induce an effective uniaxial anisotropy along the major axis of the nanomagnet.

Then, it is possible to derive a system of equations for \mathbf{m} and $\boldsymbol{\psi}_i$ (to second order in $\boldsymbol{\psi}_i$). The equation for $\boldsymbol{\psi}_i$ is cumbersome and thus omitted here as it is not necessary to the discussion that follows. That of \mathbf{m} reads

$$\begin{aligned} \frac{d\mathbf{m}}{d\tau} \simeq & \mathbf{m} \times \frac{2}{\mathcal{N}} \sum_i k_i (m_z + \psi_{z,i} - m_z \psi_i^2) \mathbf{e}_z \\ & + \mathbf{m} \times \frac{2}{\mathcal{N}} \sum_i k_i \left[\frac{1}{\mathcal{N}} \sum_j \left(m_z \frac{\psi_j^2}{2} \right) \right] \mathbf{e}_z \\ & - \mathbf{m} \times \frac{2}{\mathcal{N}} \sum_i k_i \left[(m_z)^2 + m_z \psi_{z,i} \right] \boldsymbol{\psi}_i. \end{aligned} \quad (13)$$

First, setting $\boldsymbol{\psi}_i = \mathbf{0}$ above we obtain $d\mathbf{m}/d\tau = \mathbf{m} \times \frac{1}{\mathcal{N}} \sum_i (2k_i) m_z \mathbf{e}_z = \mathbf{m} \times 2k_{\text{eff}} m_z \mathbf{e}_z$, which describes the precession of \mathbf{m} around the effective field \mathbf{h}_{eff} with

$$\mathbf{h}_{\text{eff}} = 2k_{\text{eff}} m_z \mathbf{e}_z, \quad k_{\text{eff}} = \frac{\mathcal{N}_c k_c + \mathcal{N}_s k_s}{\mathcal{N}}. \quad (14)$$

This clearly shows that nutation disappears in the absence of the spin fluctuations $\boldsymbol{\psi}_i$. Furthermore, projection on the z axis of Eq. (13) yields the relation

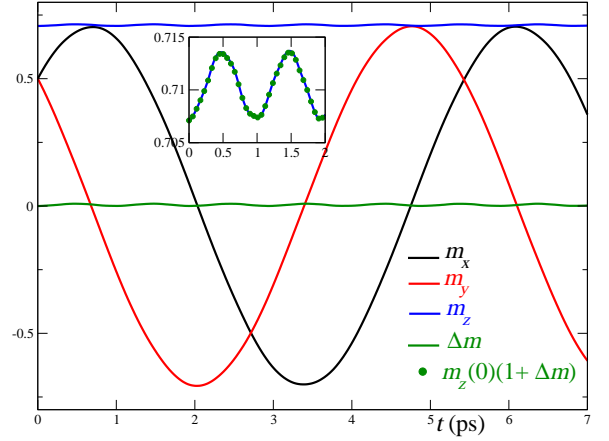


Figure 3: Time evolution of the net magnetic moment compared with that of the magnetization deficit. The exchange parameters are homogeneous ($J = J_{cs} = J_s = 1$), both surface and core spins have a uniaxial anisotropy along the z axis with surface anisotropy $k_s = 0.1$ and core anisotropy $k_c = 0.01$.

$dm_z/d\tau \simeq m_z d(\Delta m)/d\tau$, where Δm is the magnetization deficit defined in Eqs. (9, 10). Upon integrating over time we obtain (to lowest order in $\boldsymbol{\psi}_i$)

$$m_z(\tau) \simeq m_z(0) [1 + \Delta m(\tau)]. \quad (15)$$

This expression shows that $m_z(\tau)$ and $\Delta m(\tau)$ have the same frequency, as confirmed by the green dots in the inset of Fig. 3.

Therefore, this simplified model emphasizes the appearance of two relevant frequencies: the low-frequency of the ordinary precession and the higher frequency of nutation related with spin fluctuations at the atomic level driven by the exchange coupling. These two frequencies clearly show up in Fig. 1 (blue wiggles in m_z). Furthermore, in Eq. (13) we also see that the spin fluctuations $\boldsymbol{\psi}_i$ are directly coupled to the anisotropy parameters k_i , and this implies that the nutation's magnitude is not only related to the ratio of surface-to-core spin number, but also to the value of the anisotropy constants. Note, however, that the connection between Eq. (13) and Eq. (11) is not a direct one, and one has to eliminate the fast variables $\boldsymbol{\psi}_i$, *e.g.* by integration or by making use of their equations of motion in a perturbative way.

Finally, we have systematically varied the physical parameters (J_{ij} , k_i) and studied the effect on nutation and the frequencies f_p , f_c and f_n . First, we confirm that in the absence of surface anisotropy (*e.g.* the same uniaxial anisotropy k_c for all spins), no nutation has been observed. This is a direct consequence of the fact that, in this specific case, there is no magnetic inhomogeneity in the particle that can lead to a nonuniform effective field. Second, we find that the precession frequency f_p mainly depends on k_c since all spins are parallel to each other forming a macrospin that precesses in the effective

k_c	k_s	Precession frequency	Nutation frequency
		f_p (GHz)	f_n (THz)
0.001	0.001	3.2	0
0.001	0.01	19	1
0.001	0.05	86	1
0.001	0.1	170	1
0.005	0.01	25	1
0.005	0.05	93	1
0.005	0.1	180	1
0.01	0.1	185	1

J_{cs}	J_s	Precession frequency	Nutation frequency
		f_p (GHz)	f_n (THz)
2	2	25	1.5
1	2	25	1.25
1	1	25	1
1	0.5	25	0.75
1	0.1	25	0.25
0.5	0.5	25	0.7

Table I: Precession and nutation frequencies for fixed values of the exchange couplings $J = J_{cs} = J_s = 1$ (top) and for fixed values of core and surface anisotropies $k_c = 0.005$ and $k_s = 0.01$ (bottom).

tive uniform field. In general, this would also include the shape anisotropy and the DC magnetic field. On the other hand, the frequency f_n strongly depends on the exchange coupling as can be seen in Table I.

We have also performed these calculations for a spherical nanomagnet which has a different distribution of coordination numbers than in a cube. The results are qualitatively the same but the nutation frequency f_n is higher.

B. Comparison with the macroscopic approach to magnetization nutation

As discussed in the introduction, magnetization nutation has been studied by many authors within the macroscopic approach based on Eq. (1) augmented by an inertial term proportional to the second time derivative of the (macroscopic) magnetic moment \mathbf{m} :

$$\frac{d\mathbf{m}}{d\tau} = \mathbf{m} \times \left[\mathbf{h}_{\text{eff}} - \alpha \mathbf{m} \times \mathbf{h}_{\text{eff}} - \frac{\beta}{\tau_s} \frac{d^2 \mathbf{m}}{d\tau^2} \right], \quad (16)$$

where the coefficient β is often taken proportional to the damping parameter α and to a phenomenological relaxation time τ_1 related with, *e.g.* the dynamics of the angular momentum, which is on the order of a femtosecond. In Ref. 14, it was shown that the inertial damping results from high-order contributions to the spin-orbit coupling effect and is related to the Gilbert damping through the magnetic susceptibility tensor. In the sequel, we shall use the notation $\tilde{\beta} \equiv \beta/\tau_s$ and this macroscopic model,

with the equation of motion (16) and phenomenological parameter $\tilde{\beta}$, will be referred to as the *inertial one-spin problem* (IOSP).

Solving the equation above, in the presence of a DC and AC magnetic fields, *i.e.* $\mathbf{h}_{\text{eff}} = \mathbf{h}_{DC} + \mathbf{h}_{AC}$, Olive *et al.* [29] observed two resonance peaks, the first of which corresponds to the ordinary large-amplitude precession at frequency f_p and a second resonance peak, at a much higher frequency f_n with smaller amplitude, that was attributed to the nutation dynamics. A number of other authors made similar observations by also investigating the IOSP model [16, 27, 28, 47]. In Ref. [29] it was suggested that $\omega_{\text{nutation}} = 2\pi f_n = 1/\beta$.

Let us summarize the situation. On one hand, we have the EOSP model (applicable when surface effects are not too strong) in which the dynamics of the net magnetic moment is described by the equation of motion (11). The solution to the latter only exhibits two resonance peaks with frequencies f_p and f_c . On the other hand, we have the IOSP model where the equation of motion is given by (16) (with the phenomenological parameter $\tilde{\beta}$) whose solution only provides the two resonance peaks with frequencies f_p and f_n . Now, the MSP approach, when treated in its full generality, provides us with a self-consistent scheme in which all three frequencies appear in a natural manner. In particular, it shows how nutation with the high-frequency f_n sets in, in the presence of surface effects which induce non-collinear spin configurations and generate high-frequency and small-amplitude spin-wave excitations. See, for example, a thorough study of spin-wave excitations in a nanocube in Ref. 48. However, within the MSP approach, the derivation of the equation of motion for the net magnetic moment \mathbf{m} (and the spin-wave vectors ψ_i) is too cumbersome, if not intractable. This issue will be investigated in the future. Nevertheless, in the case of a spherical nanomagnet, a Helmholtz equation was derived for the vectors ψ_i in Ref. 43, see Eq. (8) therein, which is nothing else than the propagation equation for the spin waves described by ψ_i . Now, using the expansion $\mathbf{s}_i \simeq \mathbf{m} + \psi_i$, we may infer that the exchange contribution $J\Delta\mathbf{s}_i$ is proportional to the second time derivative of \mathbf{m} and, as such, the coefficient $\beta \propto 1/J$ and thereby $\omega_{\text{nutation}} \propto J$. The exact relation will be investigated in a future work.

Nevertheless, there is a specific situation in which we can establish a clear connection between the MSP approach and the IOSP model. This is the case of weak surface effects, or equivalently, a quasi-collinear spin configuration. Indeed, under this condition, we may combine the EOSP and IOSP models and write an equation of motion whose solution renders all three frequencies, f_p , f_c and f_n . More precisely, we start from Eq. (11) with the effective field $\mathbf{h}_{\text{eff}} = 2k_2 m_z \mathbf{e}_z - 4k_4 (m_z^3 \mathbf{e}_z + m_y^3 \mathbf{e}_y + m_x^3 \mathbf{e}_x)$ and add a term similar to that in Eq. (16) with coefficient $\tilde{\beta}$,

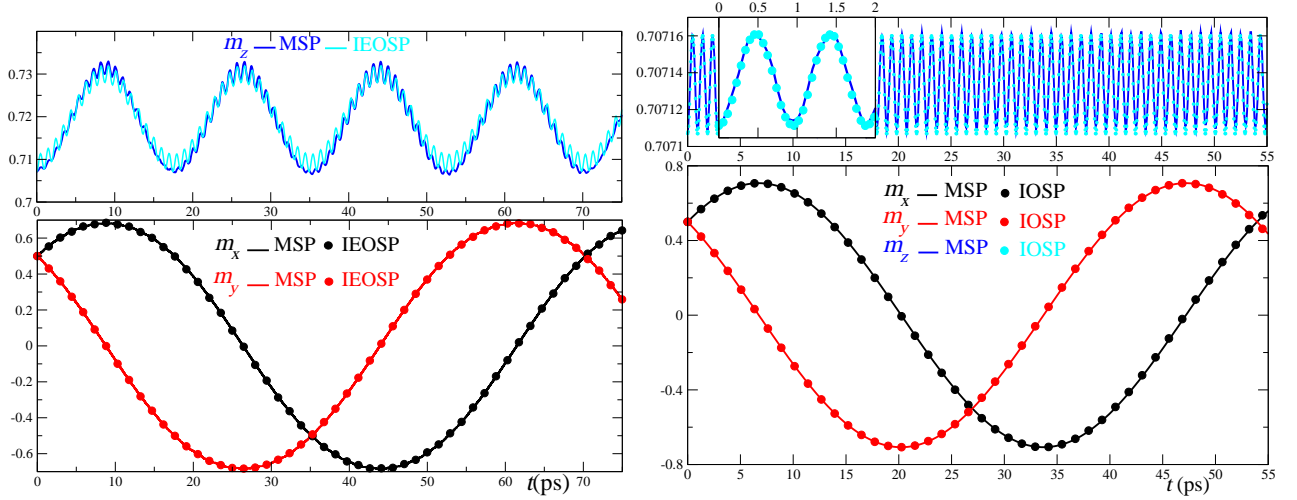


Figure 4: Time evolution of the components of the macroscopic magnetic moment \mathbf{m} (dots) and the net magnetic moment (lines) for MSP. On the left, for Néel surface anisotropy, the MSP results are compared to the IEOSP model (17) and on the right, for uniaxial anisotropy, they are compared to the IOSP model (16). The inset shows a magnification of the $m_z(t)$ component with a typical period ~ 0.9 ps ($\omega_{\text{nut}} \simeq 7$ THz).

leading to the following equation of motion

$$\frac{d\mathbf{m}}{d\tau} = \mathbf{m} \times [2k_2 m_z \mathbf{e}_z - 4k_4 (m_z^2 \mathbf{e}_z + m_y^2 \mathbf{e}_y + m_x^2 \mathbf{e}_x)] - \tilde{\beta} \mathbf{m} \times \frac{d^2 \mathbf{m}}{d\tau^2}. \quad (17)$$

where again we have $k_2 = k_c \mathcal{N}_c / \mathcal{N}$ and for a cube $k_4 = (1 - 0.7/\mathcal{N}^{1/3})^4 k_s^2 / zJ$, and $\tilde{\beta} = \beta / \tau_s$. Henceforth, this model will be referred to as the *inertial effective one-spin problem* (IEOSP).

Compared with Eq. (16), the field \mathbf{h}_{eff} has been replaced in Eq. (17) by the effective field produced by the combined uniaxial and cubic anisotropies, induced by relatively weak surface effects. Of course, we could also include an external magnetic field and a demagnetizing field in the EOSP equation. The advantage of the IEOSP model is twofold: i) it renders the three resonance peaks at the frequencies f_p , f_c and f_n and ii) it allows us to establish a clear connection between the phenomenological parameter $\tilde{\beta}$ and the atomistic physical parameters of the MSP approach, such as the surface anisotropy constant k_s .

For solving Eq. (17) one needs to set the initial velocity for \mathbf{m} . For Néel's anisotropy, the system exhibits several different velocities, depending on the spin position in the structure (edge, corner, face or core). In this case, one would have to setup a global constraint by imposing an initial velocity for the net magnetic moment (6). In practice, we have found it sufficient to use the average velocity $\dot{\mathbf{m}}(t=0) = \sum_i \dot{\mathbf{s}}_i(t=0) / \mathcal{N}$. The solution of Eq. (17) is plotted (in dots) in Fig. 4 (left).

In Fig. 4 we show the results from the MSP, IOSP and IEOSP models. The parameters for the MSP calculations

are the same as in Fig. 1, *i.e.* $k_c = 0.001$, $k_s = 0.01$. On the left, we compare the MSP approach to the IEOSP model Eq. (17) with $k_2 = 0.00475$, $k_4 = 0.0011$, $\tilde{\beta} = 2.25$. On the right, the MSP approach is compared to the IOSP model (16) with the effective field given in Eq. (14) and parameters $k_{\text{eff}} = 0.00576$, $\tilde{\beta} = 2.2$. Note that instead of using the expression for k_{eff} in Eq. (14) one might perform a fitting to the MSP curves. Doing so, we find a slight discrepancy in k_{eff} (here 0.00585) as well as in the initial velocities $\dot{m}_\alpha(t=0)$, $\alpha = x, y, z$. This is most likely due to the fact that the velocity average does not exactly account for the spin non-collinearities. All in all, the results from the MSP approach are in very good agreement with those rendered by the macroscopic model, either IOSP or IEOSP, upon using the corresponding effective field for the given anisotropy configuration in MSP, namely (12) or (3), respectively. In Fig. 4 (left), the MSP approach with the anisotropy model (3) is in good agreement with the IEOSP model with a given parameter $\tilde{\beta}$. Both models exhibit the three frequencies f_p , f_c and f_n . Regarding the nutation with frequency f_n , there is a slight discrepancy in amplitude between the two models. As mentioned above, this is attributed to the average over the initial velocities. In Fig. 4 (right) we see that, for MSP with the anisotropy model (12), the IOSP model (16) with the effective field (14), recovers the two resonance peaks with f_p and f_n . We draw attention of the reader to the difference in time scale and amplitude for the z component. Indeed, the oscillations of the z component on the right are to be identified with the wiggles of the same component on the left panel. In Ref. [29] the authors argued that $\omega_{\text{nutation}} = 1/\beta$. Here, from Fig. 4 (right) we extract $\beta \simeq 1.43 \times 10^{-13}$ s which should be compared to $\tilde{\beta}\tau_s \simeq 1.5 \times 10^{-13}$ s, showing a

good agreement.

Finally, the major difference between the results on the left and right panels is related with the frequency f_c . This implies that the model with uniaxial anisotropy, same easy axis but different constants in the core and the surface, cannot account for this frequency. This confirms the fact that the latter is related with the inhomogeneity of the on-site anisotropy easy direction and thereby with the cubic effective anisotropy as a first correction to surface effects.

In general, the relation between $\tilde{\beta}$ and the frequency f_n , within the MSP approach, is difficult to derive analytically since $\tilde{\beta}$ depends on the atomic parameters. Nevertheless, we have tried to establish a quantitative correspondence between the phenomenological parameter $\tilde{\beta}$ and the microscopic parameters such as k_s, k_c or the effective parameters k_2, k_4 that appear in Eq. (11). Accordingly, in Fig. 5 we plot $1/\tilde{\beta}$ as the result of the best fit between the MSP and IEOSP models. On the right panel of Fig. 5, this is done for the uniform uniaxial anisotropy model (12) and on the left panel for the anisotropy model in Eq. (3). These results show that $1/\tilde{\beta}$ is nearly linear in k_s and that the value of the phenomenological parameter $\tilde{\beta}$ involved in the IEOSP model can be estimated for a given value of the surface anisotropy constant k_s , which is an input parameter of the MSP approach.

Finally, we have investigated the effect of damping with parameter α [see Eq. (4)] within the MSP approach. The results are shown in Fig. 6 for the magnetization deficit. Together with the 3D picture in Fig. 2, this indicates how the spin fluctuations and thereby Δm decays in time towards zero. This result is obviously in agreement with those of Fig. 1(b) in Ref. 21. We would like to emphasize, though, that the IOSP approach in its actual formulation cannot account for the magnetization nutation in the absence of damping because the coefficient β appearing in Eq. (16) before the inertial term $d^2\mathbf{m}/dt^2$ is proportional to damping and thus vanishes when the latter does. This is one of the major discrepancies with the MSP approach since the latter does produce magnetization nutation even in the absence of such a damping ($\alpha = 0$). However, within the MSP approach the surface-induced nutation is due to local spin fluctuations and is thus affected by the spin-spin correlations or multi-magnon processes which cause damping effects and relaxation of the magnetization deficit. But in the absence of a coupling of the spin subsystem to the lattice, referred to in Ref. [49] as the direction relaxation, these damping effects are not dealt with in this work and this is why when we set $\alpha = 0$ the time evolution of m_α or Δm is undamped, but does exhibit nutation.

III. CONCLUSION AND PERSPECTIVES

We have proposed an atomistic approach for studying the effects of surface anisotropy and investigating nutation in the magnetization dynamics in ferromagnetic nanoparticles. We have then shown that because of these effects, which induce spin noncolinearities leading to nonuniform local effective fields, the magnetization dynamics exhibits several resonance peaks. In addition to the ordinary precessional motion with frequency $f_p \sim 10$ GHz, we have shown that the dynamics of the net magnetic moment exhibits two more resonance peaks with frequencies f_c and f_n which are higher than the FMR frequency. Indeed, $f_c = 4 \times f_p \sim 40$ GHz is related with the oscillations of the particle's magnetic moment between the minima of the effective potential induced by weak surface anisotropy. On the other hand, the much higher frequency $f_n \sim 1$ THz is attributed to the magnetization fluctuations at the atomic level driven by exchange coupling which becomes relevant in the presence of strong nonuniform spin configurations.

We have compared our results on nutation induced by surface effects with those rendered by the macroscopic approach based on the Landau-Lifshitz-Gilbert equation augmented by an inertial term (proportional to the second-order time derivative of the macroscopic moment) with a phenomenological coefficient. The good agreement between the two models makes it possible to estimate this coefficient in terms of the atomistic parameters such as the surface anisotropy constant. In brief, the atomistic approach provides a new origin for the magnetization nutations and a global and a self-consistent picture that renders all three frequencies.

In the case of not-too-strong surface effects, an effective model renders two frequencies f_p and f_c . On the other hand, the Landau-Lifshitz-Gilbert equation with an inertial term only renders the frequencies f_p and f_n . Now, in the case of arbitrary surface effects, it is a rather difficult task to derive an effective equation of motion for the magnetization dynamics. As such, we have proposed an intermediate model that starts from the effective model established for weak surface effects and added magnetization inertia through the term proportional to second-order time derivative of the magnetization. Then, we have shown that this macroscopic model is in very good agreement with the atomistic approach and renders all resonance peaks and their frequencies. This establishes a clear quantitative connection between the phenomenological parameters of the macroscopic approach to the atomistic energy parameters.

Our final word is devoted to the possibility of experimental observation of nutation in magnetization dynamics. First of all, establishing the fact that surface effects do induce magnetization nutation may provide us with an additional means for observing the latter. Indeed, sur-

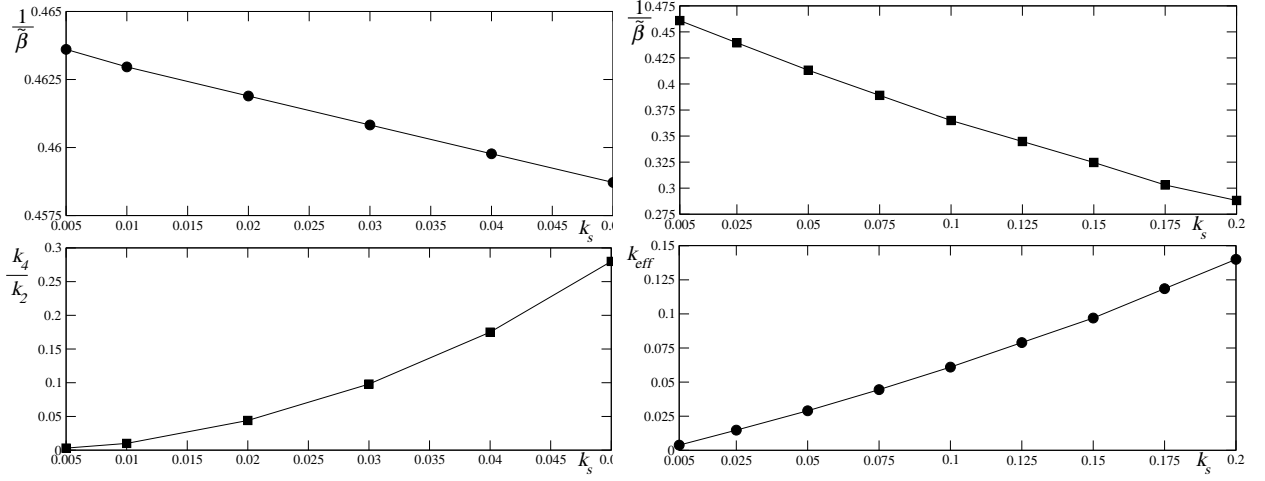


Figure 5: Left: k_4/k_2 and $1/\tilde{\beta}$ against k_s . Right: k_{eff} and $1/\tilde{\beta}$ against k_s .

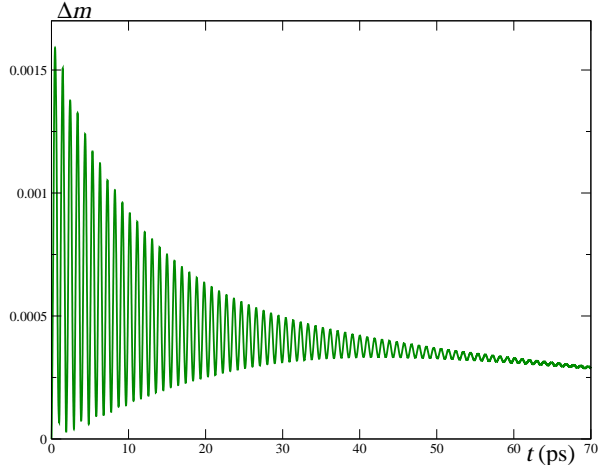


Figure 6: Time evolution of the magnetization deficit, showing the damping effect. Same parameters as in Fig. 1.

face effects on ferromagnetic resonance in nanoparticles have been studied for a few decades now. For example, the authors of Ref. 26 reported on high-frequency FMR (115–345 GHz) spectra for ultra-fine cobalt particles and inferred rather small values of the transverse relaxation time τ_{\perp} which suggests that this should be due to an inhomogeneous precession caused by (relatively weak) surface spin disorder. There are several other publications on FMR measurements on magnetic nanoparticles [50–55]. However, these measurements can only capture the two frequencies f_p and f_c . Nevertheless, the observation of the frequency f_c , which is on the order of tens of GHz, should be an easy matter using a network analyzer with variable frequency covering this range. Doing so would clearly prove the existence of the first nutation motion induced by spin disorder as a consequence of surface anisotropy. A variant of the FMR spectroscopy, called Magnetic Resonance Force Microscopy [56–58], yields a

highly sensitive local probe of the magnetization dynamics and consists in mechanically detecting the change in the longitudinal fluctuations of the magnetization, *i.e.* Δm_z . This would be particularly suited for detecting the fluctuations in m_z seen in Figs. 1 and 4, if not for the mismatch in the frequency range. Now, the frequency f_n is rather in the optical range and we wonder whether the corresponding oscillations could be detected by coupling the magnetization of the nanoparticle to a plasmonic nanoparticle of gold or silver, thus making use of the magneto-plasmonic coupling evidenced in many hybrid nanostructures [59–61]. Graphene plasmons is another promising route for detection of THz radiation [62].

We would like to acknowledge useful discussions with J.-E. Wegrowe on their early work on magnetization nutation.

* Electronic address: roland.bastardis@univ-perp.fr

† Electronic address: francois.vernay@univ-perp.fr

‡ Electronic address: hamid.kachkachi@univ-perp.fr

- [1] L. D. Landau and E. M. Lifshitz, Phys. Z. Sowjetunion **8**, 153 (1935).
- [2] T. L. Gilbert, Ph.D. thesis, Illinois Institute of Technology, Chicago (1956).
- [3] T. L. Gilbert, IEEE Transactions on Magnetics **40**, 3443 (2004), ISSN 0018-9464.
- [4] H. C. Torrey, Phys. Rev. **76**, 1059 (1949).
- [5] N. C. Verma and R. W. Fessenden, J. Chem. Phys. **58**, 2501 (1973).
- [6] P. W. Atkins, A. J. Dobbs, and K. A. McLauchlan, Chem. Phys. Lett. **25**, 105 (1974).
- [7] G. B. Hocker and C. L. Tang, Phys. Rev. Lett. **21**, 592 (1968).
- [8] G. G. Fedoruk, J. Appl. Spectroscopy **69**, 161 (2002).
- [9] J.-X. Zhu and J. Fransson, Journal of Physics: Condensed Matter **18**, 9929 (2006), URL <http://stacks.iop.org/0953-8984/18/i=43/a=014>.

- [10] J. Fransson and J.-X. Zhu, New Journal of Physics **10**, 013017 (2008), URL <http://stacks.iop.org/1367-2630/10/i=1/a=013017>.
- [11] J. Fransson, Nanotechnology **19**, 285714 (2008), URL <http://stacks.iop.org/0957-4484/19/i=28/a=285714>.
- [12] Z. Nussinov, A. Shnirman, D. P. Arovas, A. V. Balatsky, and J. X. Zhu, Phys. Rev. B **71**, 214520 (2005), URL <https://link.aps.org/doi/10.1103/PhysRevB.71.214520>.
- [13] J.-X. Zhu, Z. Nussinov, A. Shnirman, and A. V. Balatsky, Phys. Rev. Lett. **92**, 107001 (2004), URL <https://link.aps.org/doi/10.1103/PhysRevLett.92.107001>.
- [14] R. Mondal, M. Berritta, A. K. Nandy, and P. M. Oppeneer, Phys. Rev. B **96**, 024425 (2017), URL <https://link.aps.org/doi/10.1103/PhysRevB.96.024425>.
- [15] S. Bhattacharjee, L. Nordström, and J. Fransson, Phys. Rev. Lett. **108**, 057204 (2012), URL <https://link.aps.org/doi/10.1103/PhysRevLett.108.057204>.
- [16] M. Fähnle, D. Steiauf, and C. Illg, Phys. Rev. B **84**, 172403 (2011), URL <https://link.aps.org/doi/10.1103/PhysRevB.84.172403>.
- [17] T. Kikuchi and G. Tatara, Phys. Rev. B **92**, 184410 (2015), URL <https://link.aps.org/doi/10.1103/PhysRevB.92.184410>.
- [18] Thonig D., Eriksson O., Pereiro M., Scientific Reports **7**, 931 (2017).
- [19] R. Cheng, X. Wu, and D. Xiao, Phys. Rev. B **96**, 054409 (2017).
- [20] M.-C. Ciornei, J. M. Rubi, and J. E. Wegrowe, Phys. Rev. B **83**, 020410 (2011).
- [21] E. Olive, Y. Lansac, and J. E. Wegrowe, Appl. Phys. Lett. **100**, 192407 (2012).
- [22] E. Olive, Y. Lansac, M. Meyer, M. Hayoun, and J.-E. Wegrowe, Journal of Applied Physics **117**, 213904 (2015), <https://doi.org/10.1063/1.4921908>, URL <https://doi.org/10.1063/1.4921908>.
- [23] E. Olive and J. E. Wegrowe, J. Phys.: Condens. Mat. **28**, 106001 (2016).
- [24] D. Böttcher and J. Henk, Phys. Rev. B **86**, 020404 (2012).
- [25] D. A. Garanin and H. Kachkachi, Phys. Rev. Lett. **90**, 065504 (2003), URL <http://link.aps.org/doi/10.1103/PhysRevLett.90.065504>.
- [26] M. Respaud, M. Goiron, J. M. Broto, F.H. Yang, T. Ould Ely, C. Amiens, and B. Chaudret, Phys. Rev. B **59**, R3934 (1999).
- [27] Y. Li, A.-L. Barra, S. Auffret, U. Ebels, and W. E. Bailey, Phys. Rev. B **92**, 140413 (2015), URL <https://link.aps.org/doi/10.1103/PhysRevB.92.140413>.
- [28] M.-C. Ciornei, J. M. Rubi, and J.-E. Wegrowe, Phys. Rev. B **83**, 020410 (2011), URL <https://link.aps.org/doi/10.1103/PhysRevB.83.020410>.
- [29] E. Olive, Y. Lansac, and J.-E. Wegrowe, Applied Physics Letters **100**, 192407 (2012), <https://doi.org/10.1063/1.4712056>, URL <https://doi.org/10.1063/1.4712056>.
- [30] L. Néel, J. Phys. Radium **15**, 225 (1954), URL <https://doi.org/10.1051/jphysrad:01954001504022500>.
- [31] D. A. Garanin and H. Kachkachi, Magnetization reversal via internal spin waves in magnetic nanoparticles, Phys. Rev. B **80**, 014420 (2009).
- [32] E. Snoeck, C. Gatel, L. M. Lacroix, T. Blon, S. Lachaize, J. Carrey, M. Respaud, and B. Chaudret, Nano Letters **8**, 4293 (2008).
- [33] A. V. Trunova, R. Meckenstock, I. Barsukov, C. Hassel, O. Margeat, M. Spasova, J. Lindner, and M. Farle, Journal of Applied Physics **104**, 093904 (2008).
- [34] F. Jiang, C. Wang, Y. Fu, and R. Liu, Journal of Alloys and Compounds **503**, L31 (2010), ISSN 0925-8388.
- [35] B. Mehdaoui, A. Meffre, L.-M. Lacroix, J. Carrey, S. Lachaize, M. Gougeon, M. Respaud, and B. Chaudret, J. Magn. Magn. Mater. **322**, L49 (2010).
- [36] F. Kronast, N. Friedenberger, K. Ollefs, S. Gliga, L. Tati-Bismaths, R. Thies, A. Ney, R. Weber, C. Hassel, F. M. Römer, et al., Nano Letters **11**, 1710 (2011).
- [37] C. O'Kelly, S. J. Jung, A. P. Bell, and J. J. Boland, Nanotechnology **23**, 435604 (2012).
- [38] K.B. Urquhart, B. Heinrich, J.F. Cochran, A.S. Arrott, and K. Myrtle, Ferromagnetic resonance in ultrahigh vacuum of bcc Fe(001) films grown on Ag(001), J. Appl. Phys. **64**, 5334 (1988).
- [39] R. Skomski and J.M.D. Coey, Permanent Magnetism, Studies in Condensed Matter Physics Vol. 1 (IOP Publishing, London, 1999).
- [40] R. Perzynski and Yu.L. Raikher, in Surface effects in magnetic nanoparticles, edited by D. Fiorani (Springer, Berlin, 2005), p. 141.
- [41] H. Kachkachi and E. Bonet, Surface-induced cubic anisotropy in nanomagnets, Phys. Rev. B **73**, 224402 (2006).
- [42] R. Yanes, O. Fesenko-Chubykalo, H. Kachkachi, D.A. Garanin, R. Evans, R. W. Chantrell, Effective anisotropies and energy barriers of magnetic nanoparticles within the Néel's surface anisotropy, Phys. Rev. B **76**, 064416 (2007).
- [43] H. Kachkachi, Effects of spin non-collinearities in magnetic nanoparticles, J. Magn. Magn. Mater. **316**, 248 (2007).
- [44] D. A. Garanin, ArXiv e-prints (2018), 1803.10406, URL <https://arxiv.org/abs/1803.10406>.
- [45] N. C. et al., Nano Letters **1**, 565 (2001), <https://doi.org/10.1021/nl0100522>, URL <https://doi.org/10.1021/nl0100522>.
- [46] I. S. Camara, C. Achkar, N. Liakakos, A. Pierrot, V. Pierron-Bohnes, Y. Henry, K. Soulantica, M. Respaud, T. Blon, and M. Bailleul, **109**, 202406 (2016).
- [47] D. Böttcher and J. Henk, Phys. Rev. B **86**, 020404 (2012), URL <https://link.aps.org/doi/10.1103/PhysRevB.86.020404>.
- [48] R. Bastardis, F. Vernay, D. A. Garanin, and H. Kachkachi, J. Phys. C: Condens. Matter **29**, 025801 (2017).
- [49] H. Suhl, IEEE Trans. Magn. **34**, 1834 (1998).
- [50] F. Gazeau, J. C. Bacri, F. Gendron, R. Perzynski, Yu. Raikher, and V. I. Stepanov, E. Dubois, J. Magn. Magn. Mater. **186**, 175 (1998).
- [51] V. Shilov, Yu. Raikher, J.-C. Bacri, F. Gazeau, and R. Perzynski, Phys. Rev. B **60**, 11902 (1999).
- [52] D. S. Schmool and M. Schmalzl, J. Non-Crystalline Solids **353**, 738 (2007).
- [53] C. Schoepfner, K. Wagner, S. Stienen, R. Meckenstock, M. Farle, R. Narkowicz, D. Suter, and J. Lindner, Journal of Applied Physics **116**, 033913 (2014).
- [54] K. Ollefs, R. Meckenstock, D. Spoddig, F. M. Römer, C. Hassel, C. Schöppner, V. Ney, M. Farle, and A. Ney, Journal of Applied Physics **117**, 223906 (2015).
- [55] I. S. Poperechny and Yu. Raikher, Phys. Rev. B **93**, 014441 (2016).

- [56] J. A. Sidles, J. L. Garbini, K. J. Bruland, D. Rugar, O. Züger, S. Hoen, and C. S. Yannoni, *Rev. Mod. Phys.* **67**, 249 (1995), URL <http://link.aps.org/doi/10.1103/RevModPhys.67.249>.
- [57] B. Pigeau et al., *Phys. Rev. Lett.* **109**, 247602 (2012).
- [58] Lavenant, H., Naletov, V. V. Klein, O. De Loubens, G. Laura, C. De Teresa, J. M., *Nanofabrication* **1**, 65 (2014).
- [59] J. B. Gonzalez-Diaz, A. Garcia-Martin, J. M. Garcia-Martin, A. Cebollada, G. Armelles, B. Sepulveda, Y. Alaverdyan, and M. Kall, *Small* **4**, 202 (2008), URL <https://onlinelibrary.wiley.com/doi/abs/10.1002/sml1.200700>.
- [60] V. V. Temnov et al., *Nature Photonics* **4**, 107 (2010).
- [61] A. Gaspar, C. Alfonso, G.-M. Antonio, and G. M. Ujue, *Advanced Optical Materials* **1**, 10 (2013), URL <https://onlinelibrary.wiley.com/doi/abs/10.1002/adom.201200>.
- [62] D. A. Bandurin, D. Svintsov, I. Gayduchenko, S. G. Xu, A. Principi, M. Moskotin, I. Tretyakov, D. Yagodkin, S. Zhukov, T. Taniguchi, et al., *ArXiv e-prints* (2018), 1807.04703.